

Research article

Analysis of the impact of offshore wind power on the Japanese energy grid

YingTung Chen, Kristina Knüpfer, Miguel Esteban* and Tomoya Shibayama

Department of Civil and Environmental Engineering, Waseda University, 3-4-1 Okubo, Shinjuku-ku, 169-8555 Tokyo, Japan

* **Correspondence:** Email: esteban.fagan@gmail.com; Tel: +81-8040267791.

Abstract: As part of its economy-wide decarbonization target towards 2050, Japan plans to increase renewable generation, especially offshore wind, for which the country has a high potential. However, this resource is currently under-developed as available turbines are prone to shut-downs and can even suffer damage during the passage of typhoons. With new typhoon proof (T-class) turbines being currently developed by various companies, Japan now aims to develop 10 GW of offshore wind between 2021 and 2030, and 91 GW in the long-term. This research estimates the impact of integrating offshore wind into the Japanese main power grid using T-class turbines by considering three scenarios. First, a business-as-usual (BAU) case with 10 GW offshore wind capacity (following the 6th Strategic Energy Plan of Japan). Second, an offshore wind capacity of 91 GW. Third, the 91 GW offshore capacity being redistributed amongst regions to maximize its integration opportunities (Scenario 2). The simulations were carried out using the Energy System simulation model (EnSym). The results show that the BAU and Scenario 1 resulted in offshore wind achieving 1.7% and 7.28% of generation share, respectively, increasing to 9.77% for Scenario 2. Increasing the share of offshore wind in the energy mix mainly replaced liquefied natural gas (LNG).

Keywords: offshore wind; T-class turbine; renewable energy mix; typhoon; energy system modelling; Japan

Highlights

- Increased offshore wind mainly replaces LNG generation.
- Offshore wind improved overall demand coverage compared to LNG.
- Offshore wind shares were maximized through development near high-demand regions.

1. Background

To mitigate the adverse effects of anthropogenic climate change, the United Nations Framework Convention on Climate Change (UNFCCC) established the Paris Agreement to regulate CO₂ emissions [1], as these contributed 76% of global greenhouse gas emissions [2]. As a result, governments around the world that signed the agreement are currently attempting to decarbonize their economies.

Through its energy sector decarbonization strategy, the Japanese government aims to achieve zero CO₂ emissions by 2050 [3]. To do this, the government regularly formulates Strategic Energy Plans (SEP) updated approximately every 3 years, and currently in its 6th revision [4], which are led by three principles, namely efficient supply, energy security and environmental protection, supported by the condition of safe operation [5]. Mid-term targets include the reduction of greenhouse gas emissions by 26% from 2013 levels by 2030, and to achieve a 25% self-sufficiency ratio (Defined as the ration of energy produced from domestic sources and that imported from overseas) by this date [5], up from 20.3% in 2010, and 11.6% following the *2011 Tohoku Earthquake and Tsunami* (11.2% as of 2021[6]).

To achieve these targets, the 6th SEP has set more ambitious targets for renewable sources for electricity (RES-E) than the 5th SEP, increasing total RES-E target shares from 22~24% to 36~38% for 2030, and prioritizing and maximizing renewable energy integration (see Table 1).

Table 1. Projected energy mix in 2030 according to the 5th and 6th SEP.

	Nuclear	LNG	Coal	Oil	Hydrogen	Solar	Wind	Geothermal	Hydropower	Biomass
5 th SEP	20~22%	27%	26%	3%	0%	7%	1.7%	1~1.1%	8.8~9.2%	3.8~4.6%
6 th SEP	20~22%	20%	19%	2%	1%	14~16%	5%	1%	11%	5%

The focus of the 6th SEP is to decrease the share of fossil fuels in electricity generation, while doubling solar PV and almost tripling the wind share. The government of Japan aims to achieve the latter by not only increasing the installed onshore wind capacity but also by newly introducing 10 GW of offshore wind, thereby increasing the wind resource overall by 19.7 GW compared to 2021 (4.6 GW). Indeed, while wind has not played an important role in the Japanese energy mix until now, offshore wind capacity is planned to be developed in three stages between 2030 (10 GW), 2040 (30~45 GW) and 2050 (90 GW) to achieve carbon neutrality [7], as well as enhance domestic self-sufficiency [5]. The distribution of the planned capacities by region is summarized in Table 2.

Table 2. Regional distribution of offshore wind capacity (GW) by year.

	Total	Hokkaido	Tohoku	Kanto	Chubu	Hokuriku	Kansai	Shikoku	Chugoku	Kyushu
2020	0.06	0.0012	0.02	0.032	0	0	0	0	0	0.005
2030	10.72	1.24	4.07	0.35	1.35	0.7	0.75	0	0.06	2.2
2040	45	14.65	9	3.7	1.35	1.3	0.9	1.7	0.5	11.9

Therefore, by 2030 wind could play a much more substantial role in the Japanese energy system than it does as of 2022. Furthermore, other than for electricity generation, wind energy is also planned to be used for hydrolysis to generate H₂ for the transport sector [8]. For this purpose, Hokkaido prefecture carried out evaluations in 2018 [9], and Kyushu prefecture conducted experiments in 2021 [10]. While plans to develop hydrolysis capacity as a collaboration between government and companies (such as Hitachi, Muroran Institute of Technology, NTT Facilities and Nagasaki industrial promotion foundation) in Hokkaido and Kyushu have been confirmed [9,10], it is unclear as of July 2022 how much hydrolysis capacity is planned in these regions.

Despite the relatively high potential of offshore wind as a domestic resource (ca. 91 GW [7]), it remains largely undeveloped as of 2022. Partially, this is due to the water depth off the east coast of Japan, which results in a high construction cost for wind turbines [11]. Further, Japan is prone to typhoons between July and October, which can force currently available turbine models to shut down and even cause severe structural damage [12,13].

To address this problem and harvest the potential energy from typhoon-strength winds, various companies have begun developing so-called “T-class” turbine models. These include the SG 11.0-200 DD by Siemens Gamesa [14], the V174-9.5 MWTM [15] and the V236-15MWTM by Vestas [16], the MySE 16.0-242 by MingYang Smart Energy [17], as well as the Haliade-X 12-14.7MW-220 by General Electric [18]. The two former turbine models had prototypes installed successfully in 2021 [19] and 2020 [20], respectively, with orders made in the Netherlands, Germany and Taiwan [21]. For V236-15MWTM, the installation of a prototype turbine is planned for the second half of 2022 and serial production by 2024 [22]. The MySE 16.0-242 is scheduled for prototype rollout in 2022, prototype installation in the first half of 2023 and commercial production in the first half of 2024 [23].

Offshore wind will likely become more important to the energy mix of Japan given the development of T-class turbines and the government’s long-term targets to support it. In this context, it is important to understand how an increase in wind capacity would affect the energy mix and which measures would be best suited to fulfill the overall Japanese energy policy targets. Energy system models can assess this impact on the energy mix and are therefore a useful tool in this context. Previous energy models have assessed the viability of various energy mixes for Japan toward 2030 [24–31] and 2050 [32,33]. These studies assess major resources such as oil, LNG, coal, nuclear, solar PV, onshore wind, biomass, geothermal, pumped hydro storage and battery storage. However, given that it was a negligible resource as of 2022, offshore wind was not considered in any such existing research regarding Japan to the best of the authors’ knowledge.

Based on the identified gaps, this work will introduce offshore wind as a major resource when simulating the energy mix in Japan for 2030, using both the projected capacity for that year, as well as the expected maximum capacity of 91 GW. In doing so, the authors aim to determine the potential contribution of offshore wind to the Japanese energy system by 2030 and in the long-term. Finally, the authors estimate whether the resource capacity distribution planned by the government of Japan can be improved, from the perspective of maximizing the integration opportunities of offshore wind into the system.

2. Methodology

2.1. Model overview

Simulations were carried out using the Energy System Simulation Model (EnSym) developed by Knüpfer *et al.* [31]. EnSym simulates all major resources including nuclear, coal, oil, LNG and renewable resources, such as hydro power, solar PV, onshore wind, biomass, and geothermal, as well as utility scale batteries and pumped hydro storage. The simulations use an hourly time-scale, and include all regions in Japan except the Ryukyu Islands, as this chain of southern Japanese islands is not connected to the main grid. EnSym takes into account inter-regional electricity transmission and can flexibly adopt different dispatch hierarchies for resources. In this study, variable renewables (e.g., wind, solar PV, and utility scale batteries and pumped hydro charged by them) were prioritised over flexible energy resources (e.g., LNG, biomass and geothermal), which were in turn prioritised over thermal resources (e.g., nuclear and coal). Nuclear power, hydro and coal act as baseloads. For a detailed overview of the model, please see Knüpfer *et al.* [31]. In the present work, the authors modified EnSym to newly introduce offshore wind power into the model. Further, the balancing procedure was improved compared to the previous version of the model.

2.2. Electricity supply

The target installed capacities for all major resources for 2030 were obtained from the most recent projection by the Ministry of Economy, Trade and Industry [34] for coal, LNG, oil, nuclear, solar, geothermal, onshore wind, offshore wind, biomass, and conventional hydropower. For these resources, previous projections for 2030 by the government of Japan were assumed to still be up-to-date [35]. Further, for any capacity with a target range, the average value was taken (see Table 3).

Table 3. Target installed capacities for all major resources for 2030 (sources: METI [34]; OCCTO [35]; ANRE [36]; JAIF [37]).

Resources	Installed capacity (GW)
Coal	51.9
LNG	84.9
Oil	30.8
Nuclear	38
Solar	87.6
Geothermal	1.4~1.6
Onshore wind	13.3~15.3
Offshore wind	1.7~3.7
Biomass	7.2
Conventional hydropower (Small-to-mid-scale)	10.94~11.65

Among the planned capacities shown in Table 3, the authors adjusted those for nuclear power, solar and offshore wind. Due to the decommissioning of existing nuclear capacity and the lack of sufficient new capacity being planned by 2030, the authors assumed that the installed capacity of nuclear power by 2030 will not exceed 33.2 GW (see Appendix for details). For solar PV, the planned capacity of 88 GW [34] seems to be an underestimation compared with the expected installed capacity for 2030 of 139.12 GW by ANRE [36] (The PV generation share targets for 2030 set by the 5th SEP were

achieved in 2020 (7%), and the capacity targets for 2020 (64 GW) have also been exceeded (136 GW, if all already approved capacity is included, see Knüpfer *et al.* [38]). Therefore, the authors adopt the latter value. For offshore wind, the planned distribution of newly developed capacities for 2030 is unclear as of July 2022. Therefore, the authors based the distribution on offshore wind projects that are currently undergoing environmental assessment [39]. The regional distribution of all other resources follows Knüpfer *et al.* [31]. Where total installed capacity volumes differ from Knüpfer *et al.* [31], the additional expected capacities were either distributed proportionately over the regions, or according to known regional development projects (see the Appendix)).

Table 4 provides an overview of the total expected capacity projected by METI [34] and the business-as-usual base case (BAU) based on amendments by the authors (“Japan realistic”), as well as the associated regional distributions (also based on the estimates by the authors).

Table 4. Installed capacity (GW) of each resource in each region of Japan in 2030 (for the BAU)

Resource	METI projection	Japan realistic	Hokkaido	Tohoku	Kanto	Chubu	Hokuriku	Kansai	Shikoku	Chugoku	Kyushu
Coal	51.9	51.9	1.9	4.3	17.3	7.5	0.8	9.6	1.9	3.3	5.3
LNG	84.9	84.9	3.1	7	28.2	12.3	1.4	15.7	3.1	5.4	8.7
Oil	30.8	30.8	1.1	2.5	10.2	4.5	0.5	5.7	1.1	2	3.1
Nuclear	38	33.2	2.1	2.8	1.1	3.6	11.3	6.5	0.9	0.8	4.1
Hydro Conventional	23.75	23.75	1.4	3.9	1.5	8	4	0.87	0.98	1.1	2
Hydro pumped	27.47	27.47	1	0.5	5.3	10.1	1.6	4	0.6	2.1	2.3
Solar PV	87.6	139.12	4.27	16.06	52.37	15.15	1.2	12.2	3.66	7.8	26.4
Onshore wind	14.3	14.3	2.2	5.2	0.46	0.7	0.47	1.39	0.7	1.28	1.86
Offshore wind	2.7	10	1.5	4.5	0.4	0	0.7	0.7	0	0	2.2
Geothermal	1.5	1.5	0.08692	0.85	0.00005	0.00057	0.00024	0.0001	0	0.00005	0.55483
Biomass	7.2	7.2	0.32	1.14	1.08	1.26	0.58	0.6	0.42	0.92	0.9

Utility scale batteries were also considered [40], with their capacity assumed to remain unchanged between 2020 and 2030 (Table 5) as no information regarding development plans could be identified. Obviously, an increase in the capacity of batteries will result in a more robust and stable system [26], and thus assuming that this remains constant represents a conservative assumption.

Table 5. Announced, commissioned and operational large-scale battery rated power (MWh) as of 2021 (Source: DOE [40]).

Storage medium	Japan	Hokkaido	Tohoku	Kanto	Chubu	Hokuriku	Kansai	Shikoku	Chugoku	Kyushu
Battery	910	73.8	323.5	180.8	0.0	0.0	2.7	0.0	25.3	303.9

To simulate the full estimated potential (91 GW) of offshore wind in Scenarios 1 and 2, the installed capacity was adjusted based on its current development plan [39]. As some regions had no

offshore wind capacity installed in the BAU, the offshore wind capacity distribution for 91 GW was based on the 2040 regional target (45 GW), which has capacity installed in every region [39], and then scaled up proportionally to reach 91 GW (see Table 6).

Table 6. Expected offshore wind regional distribution for 91 GW.

	Total	Hokkaido	Tohoku	Kanto	Chubu	Hokuriku	Kansai	Shikoku	Chugoku	Kyushu
Installed capacity (GW)	91	29.4	18.2	7.5	2.7	2.6	1.8	3.4	1.0	24.3

The hourly electricity generation potential for solar PV and onshore wind was calculated using hourly meteorological data from one measurement station per prefecture [41]. The station locations for onshore wind were adapted from Knüpfer *et al.* [31]. For offshore wind, one measurement station per region was chosen [42] (see the Appendix for all stations used), considering only those stations that were not in the wind shadow of mountains and close to the coastline. (The furthest station from the coast was 303 meters inland). For solar PV installed capacity, it was assumed that every panel was a Hanwha G5-280 series, and for offshore wind capacity that every turbine was a V236-15MWTM (see Appendix for details). It was also assumed that each offshore wind park was directly connected to the respective regional grid through typical submarine cables (see Appendix).

As for thermal resources, it was assumed that there is no requirement of maintenance throughout the year and the only output constraint is the capacity factor (see Table 7).

Table 7. Resource capacity factor (Sources: Geothermal Energy [43]; USACE [44]).

Resource	Capacity factor
Coal	0.7
Oil	0.85
LNG	0.7
Nuclear	0.9
Biomass	0.8
Geothermal	0.85

2.3. Electricity demand

This study assumes an annual electricity demand for 2030 of 1065 TWh [36]. The hourly demand profile was based on that previously estimated by Knüpfer *et al.* [31], using monthly demand values for each prefecture from 2017 [45]. The hourly time series of demand throughout the day was obtained by distributing these monthly values through a weighting factor, using as a base the hourly demand values of the Kanto region [46]. The hourly demand used in the simulation employs hourly values from the 2017 base year, and proportionately adjusted them based on the change in the expected future annual demand. For further details, please refer to Knüpfer *et al.* [31].

2.4. Scenario set-up

The present research has two aims. First, to understand the potential contribution to the energy mix that offshore wind could make by 2030 and in the long-term. Second, to estimate whether the planned long-term spatial distribution of offshore wind capacity is optimal for the maximum integration of wind into the energy system.

To achieve the first aim, a business-as-usual (BAU) and Scenario 1 were defined. The objective of the BAU was to estimate the impact of offshore wind on the energy mix based on the 2030 capacity target. Scenario 1 estimates the impact of offshore wind on the energy mix in the long-term by simulating the maximum estimated capacity of 91 GW [7], which is approximately the same as the current maximum planned capacity of 90 GW [7]. The 91 GW capacity is distributed proportionately according to current plans for 2040 [39].

To achieve the second aim, the authors assumed an installed capacity of 91 GW for offshore wind in Japan in Scenario 2 and re-distributed the planned [39] regional offshore wind capacity using the model simulation to maximize its integration potential, while keeping all other resources and transmission grid capacity constant. Table 8 summarizes the scenario settings.

Table 8. Scenario and BAU definitions, objectives and settings in the EnSym model.

Scenario	Description and objective	Installed capacity	RES-E generation share (%)
BAU	Simulate electricity generation for Japan with the expected resource shares in 2030 according to the 6 th Strategic Energy Plan	6 th SEP	6 th SEP
1	Estimate the impact of integrating the maximum offshore wind capacity for the Japanese energy mix	6 th SEP with 91GW offshore wind (regional distribution of offshore according to government of Japan)	Estimated through the simulation
2	Estimate whether offshore wind integration can be improved by adjusting regional distribution	6 th SEP with 91GW offshore wind (regional distribution of offshore optimized by model)	Estimated through the simulation

3. Results

3.1. BAU: the impact of offshore wind on the energy mix by 2030

Figure 1 shows the 6th SEP energy target for each resource in 2030, together with the simulated BAU. Compared to the 6th SEP energy mix target, oil and LNG respectively represent 1.35% and 11.52% more of the energy mix than expected, while conventional hydro, biomass, geothermal, wind and solar did not reach their target shares.

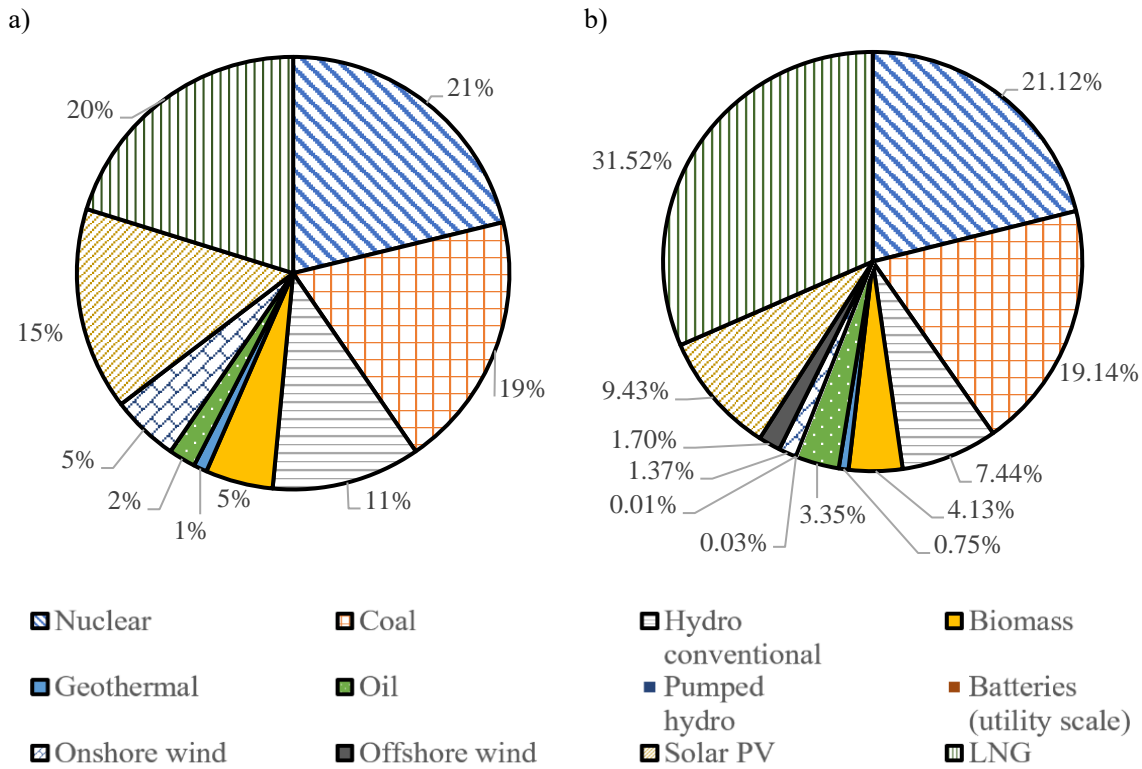


Figure 1. a) The 6th SEP target share for each resource in 2030 and b) The BAU energy mix with the planned installed capacity for each resource in 2030.

Figure 2 shows the energy mix over 24 hours on one of the highest demand days (8th August 2030) in the year for Japan.

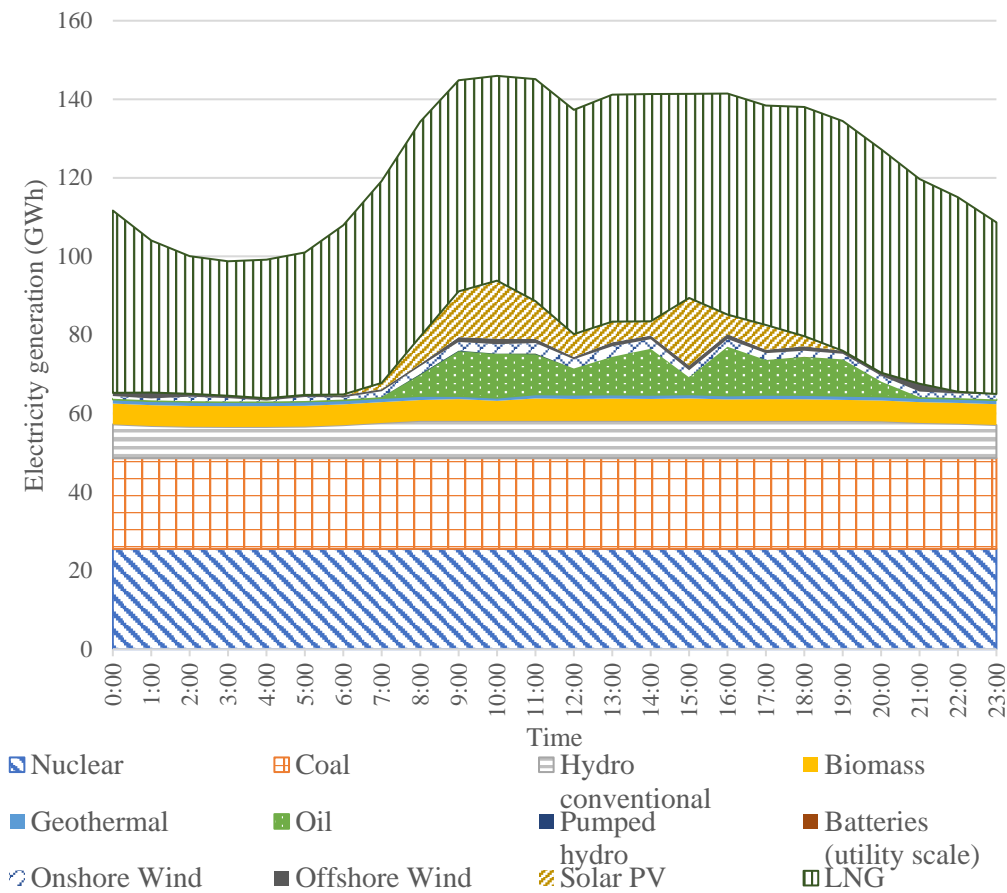


Figure 2. BAU energy mix on 8th August 2030.

Table 9 shows how some differences can be observed between the 8th August 2030 and the annual generation shares for each resource. While the overall tendency is similar to the annual energy mix, the share of offshore wind and solar PV were 0.99% and 6.4% lower, respectively. This reduction was balanced by biomass, geothermal, oil and LNG.

Table 9. Energy mix by resource on 8th August 2030 (GWh).

Nuclear	Coal	Hydro conv.	Biomass	geothermal	oil	Pumped hydro	Batteries	Onshore wind	Offshore wind	Solar PV	LNG
612.7 (20.4%)	554.4 (18.5%)	215.6 (7.20%)	129.6 (4.33%)	25.15 (0.84%)	115.9 (3.87%)	0.579 (0.02%)	0.051 (0.002%)	37.16 (1.24%)	21.15 (0.71%)	90.71 (3.03%)	1193.2 (39.8%)

3.2. Scenario 1: the 6th SEP energy mix with maximized offshore wind capacity

After obtaining the BAU energy mix, the installed capacity of offshore wind was increased from 10 to 91 GW at the country-level, and regionally distributed as described in section 2.2. The installed capacities for all other resources were kept constant. Increasing the offshore wind capacity increased the annual share of wind from 3.07% to 8.56% (see Figure 3). Further, solar PV increased by 0.28%, while the generation of all other resources (except pumped hydro and batteries), decreased as they were replaced by the increase in variable renewables.

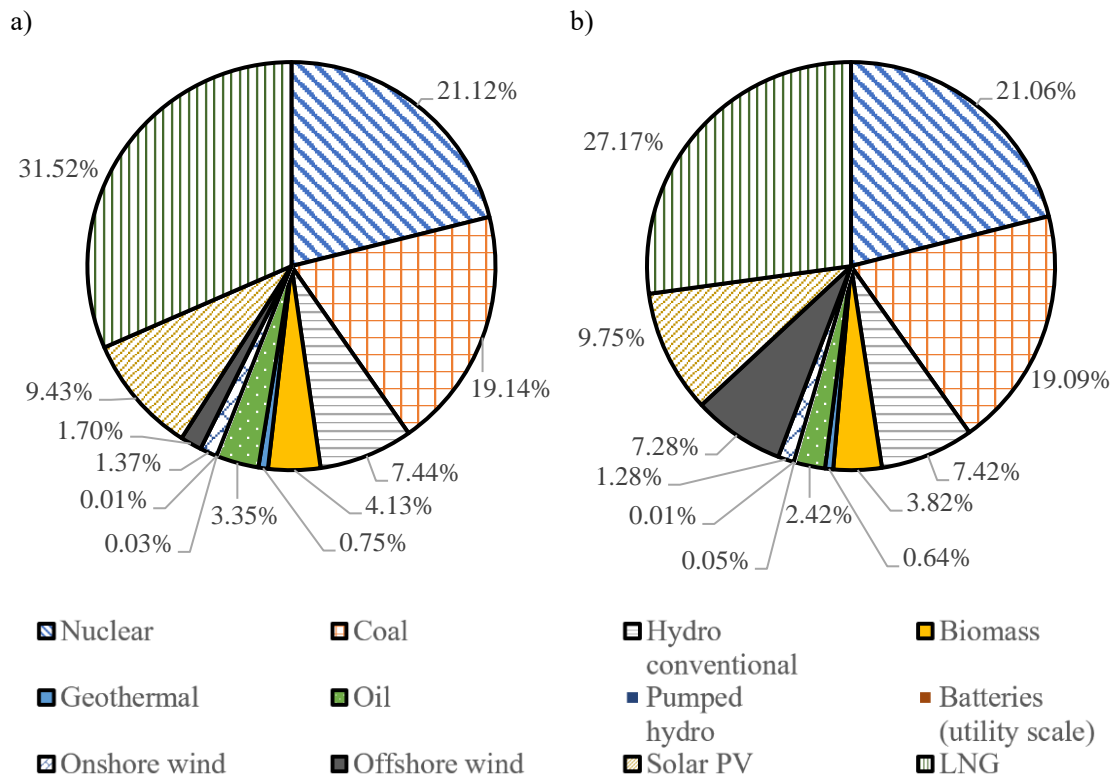


Figure 3. a) Annual energy mix for BAU and b) Scenario 1.

Figure 4 shows the energy mix for 24 hours on a high demand day in Japan (8th August 2030).

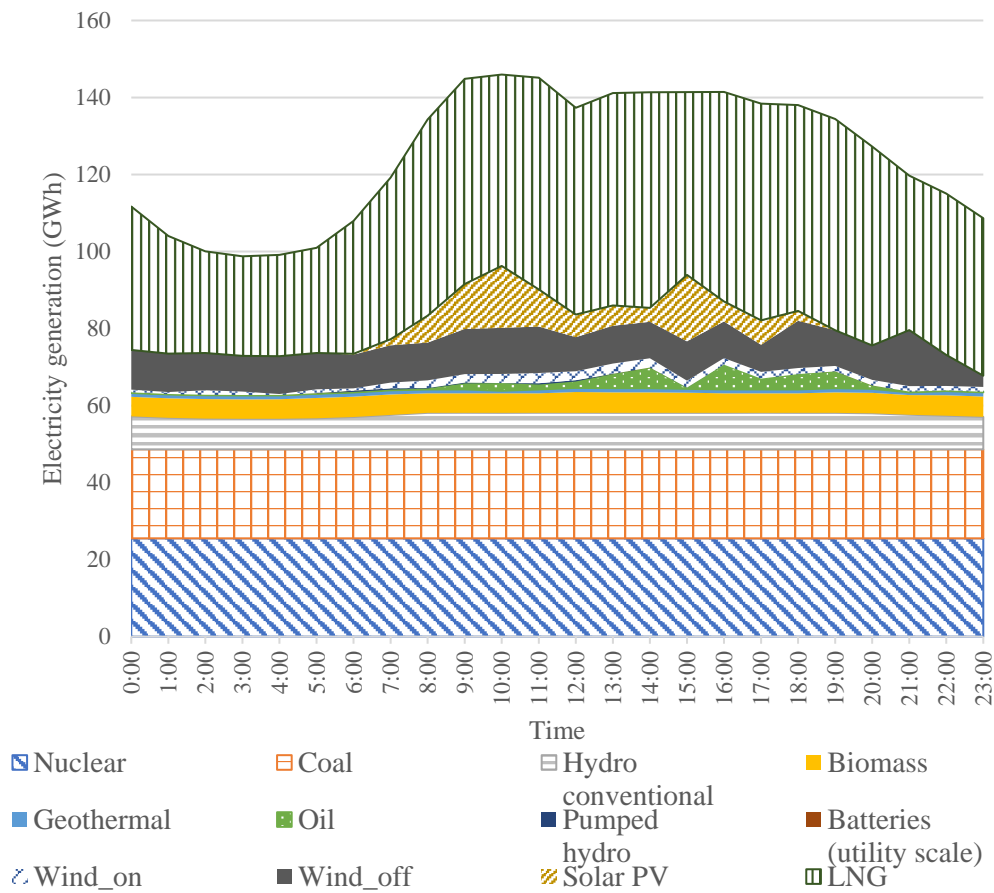


Figure 4. Scenario 1 energy mix on 8th August 2030.

Table 10 shows the respective resource generation shares for the BAU and Scenario 1 on 8th August 2030. Compared to the BAU, Scenario 1 increased offshore wind generation, replacing 208 GWh of LNG and oil generation throughout the day.

Table 10. Energy mix by resource on 8th August 2030 (GWh).

Scenario	Nuclear	Coal	Hydro convent.	Biomass	Geother mal	Oil	Pumped hydro	Batteries	Onshore wind	Offshore wind	Solar PV	LNG
BAU	612.7 (20.4%)	554.4 (18.5%)	215.6 (7.20%)	129.6 (4.33%)	25.15 (0.84%)	115.9 (3.87%)	0.579 (0.02%)	0.051 (0.002%)	37.16 (1.24%)	21.15 (0.71%)	90.71 (3.03%)	1193.2 (39.8%)
1	612.7 (20.4%)	554.4 (18.5%)	215.6 (7.20%)	123.9 (4.14%)	24.30 (0.81%)	36.07 (1.20%)	1.686 (0.06%)	0.222 (0.01%)	36.94 (1.23%)	233.2 (7.78%)	92.17 (3.08%)	1065.0 (35.5%)

3.3. Scenario 2: improving wind integration through capacity distribution

The objective of Scenario 2 was to estimate whether offshore wind integration can be improved by adjusting its planned regional distribution [39] through EnSym, while assuming that all other resource- and transmission capacities remain unchanged. Figure 5 compares resource generation shares in the energy mix between Scenarios 1 and 2.

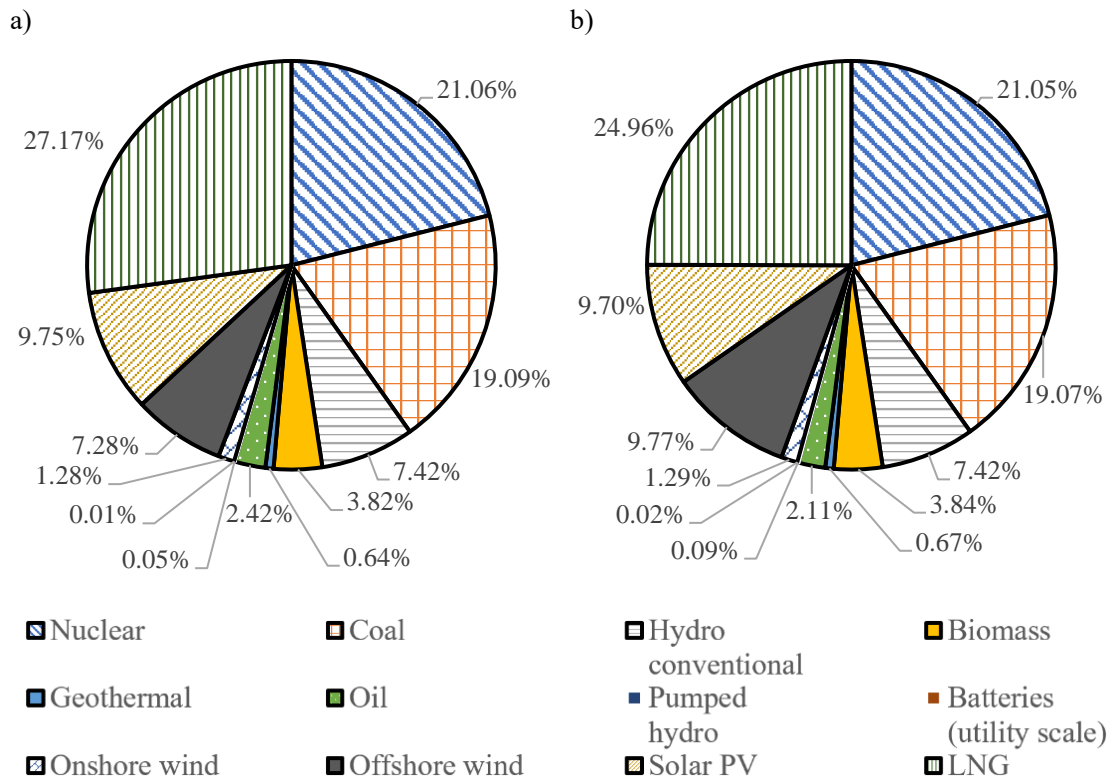


Figure 5. a) Annual energy mix for Scenario 1 and b) Scenario 2.

By adjusting the distribution of the offshore wind resource compared to the current plan [39], the share of offshore wind increased by 2.49% and overall demand coverage improved from 99.53% (Scenario 1) to 99.61% (Scenario 2), with the RES-E share increasing from 30.16% to 32.80%, mainly by replacing LNG (−2.21%), as well as some nuclear, coal, and oil.

Table 11 provides an overview of the differences in offshore wind capacity distribution between the current plan ([39]; Scenario 1) and the distribution which the authors determined through the simulation (Scenario 2). In Scenario 1 it can be observed that there is a general trend for offshore wind distribution to follow the distribution of the resource potential (mainly in Hokkaido and Kyushu) [39]. In Scenario 2 the capacity distribution estimated through the simulation for maximized integration of the resource in the energy mix focuses on development in or directly neighboring high electricity demand regions. Only Tohoku is a focus region in both Scenario 1 and Scenario 2, as it has both high resource potential in itself, as well as neighboring a high demand region (Kanto, where Tokyo is located).

Table 11. Offshore wind installed capacity regional distribution (GW).

Scenario	Total	Hokkaido	Tohoku	Kanto	Chubu	Hokuriku	Kansai	Shikoku	Chugoku	Kyushu
1	91	29.35	18.22	7.49	2.73	2.63	1.82	1.01	3.44	24.29
2	91	2	13	27.35	11.6	0.05	10	9	9	9

Figure 6 shows that, on a high demand day, the difference in the resource distribution between Scenario 1 and Scenario 2 (Table 12) is minor, with a slight tendency for biomass, oil and wind to increase.

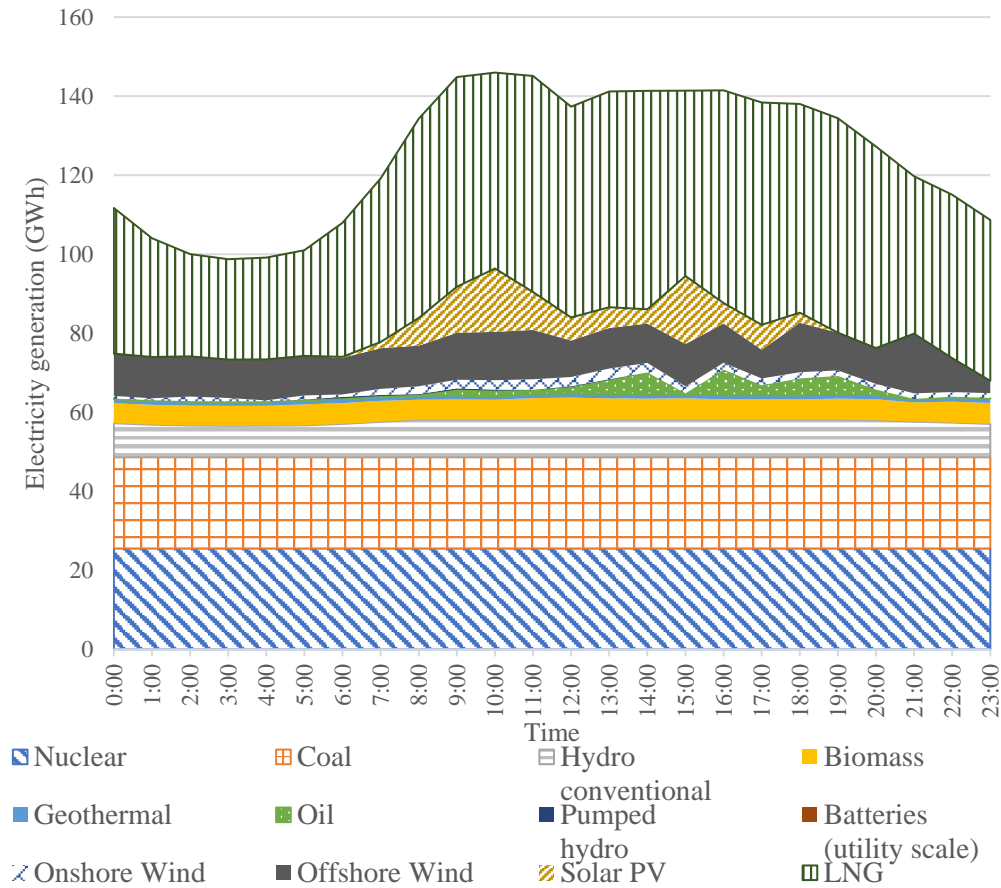


Figure 6. Scenario 2 energy mix on 8th August 2030.

Table 12. Energy mix by resource on 8th August 2030 (GWh).

Scenario	Nuclear	Coal	Hydro convent.	Biomass	Geothermal	Oil	Pumped hydro	Batteries	Onshore wind	Offshore wind	Solar PV	LNG
1	612.7	554.4	215.6	123.9	24.30	36.07	1.686	0.222	36.94	233.2	92.17	1065.0
	(20.4%)	(18.5%)	(7.20%)	(4.14%)	(0.81%)	(1.20%)	(0.06%)	(0.01%)	(1.23%)	(7.78%)	(3.08%)	(35.5%)
2	612.7	554.4	215.6	124.9	24.32	36.17	1.612	0.197	36.94	243.1	92.17	1054.1
	(20.4%)	(18.5%)	(7.20%)	(4.17%)	(0.81%)	(1.21%)	(0.05%)	(0.01%)	(1.23%)	(8.11%)	(3.08%)	(35.2%)

4. Discussion

4.1. Comparisons between scenarios

The higher share of LNG and oil in the BAU compared to the planned generation according to the 6th SEP is likely due to the relationship between the spatial distribution of the capacity of these

resources with respect to the electricity demand distribution. Both oil and LNG capacities are near the major demand centers and are flexible, meaning they can be dispatched irrespective of weather conditions (which solar PV and wind are dependent on) and at short notice. To minimize the burden on the grid, the model prefers dispatching resources as close to demand locations as possible. Therefore, during hours of low solar PV and wind availability, LNG and oil will be more likely to increase their generation than biomass, hydro or geothermal in high-demand regions which are mainly Kanto and Kansai. Lastly, assuming that enough solar PV and wind capacity are installed to technically achieve the target share, then the lack in generation observed in Figure 1 may also be due to the meteorological conditions of the base year chosen, which was 2018.

4.2. Difference in distribution strategy

The offshore wind capacity distribution between Scenario 1 (in accordance with METI [39]) and Scenario 2 (estimated by the authors through the simulation) show significant strategic differences. While the distribution aimed for by the government of Japan is focused on the resource-rich regions of Hokkaido and Kyushu, the simulation by the authors focused on the electricity demand centers of Kanto and Kansai, as well as their direct neighbors.

There are two main reasons for these differences. First, the government of Japan aims to use some of the offshore capacity in Hokkaido and Kyushu for H₂ production by water electrolysis. This would reduce the pressure on the transmission grid and could allow for the efficient use of wind generated in these regions in a way which cannot be reflected in the model's current configuration. Second, the model was more likely to prefer placing capacity in regions other than Kyushu and Hokkaido as these two regions only have limited transmission capacity between them, compared to the two or three in other regions, which provides more flexible opportunities for transmission in the simulation.

Even though the model does not currently reflect the transport sector use of wind generation capacity, the distribution estimated by the authors in Scenario 2 can serve as an indicator as to an optimized resource capacity distribution for maximized integration opportunities. This may be useful for companies planning to develop offshore wind power capacity for interconnection to the grid rather than direct H₂ production by electrolysis.

4.3. Model limitations

The model aims to match the power demand in each region for each hour with the corresponding power supply. In the present simulation, the increase in offshore wind between scenarios improved the overall demand coverage achieved (from 99.25% to 99.61%), as well as the total RES-E share (from 24.86% to 32.80%), with the latter improvement mostly being due to the increase in offshore wind (up by 8.07%), which mainly replaced LNG (down by 6.56% between the BAU and Scenario 2). The discrepancy between generation and demand (0.39% in Scenario 2) is mainly due to a compounding rounding error recorded each hour due to the categorization of variables. Removing this error should be addressed in further development of the model. The model has, while being tested during development, achieved 100% demand coverage on several occasions but this is not yet consistent. Despite this shortcoming, EnSym does improve on previous models by including several types of storage capacities (compared to Wakiyama and Kuriyama [29]), and avoiding looping issues by defining flow rules that track transmission line usage (compared to Kainou [47] and

Yoshihara and Ohashi [30]). Also, it should be noted that the model detailed here does not include the charging of electrical vehicles, hybrid cars or electrolyzers, which should be targeted in further improvements to the model. Further, EnSym does not currently distinguish between the various demand groups (for example, households, industry). In the future it would be useful to differentiate between the various demand groups, as their patterns may change and interact with renewables such as solar PV. Further, to increase the representativeness of the results, particularly related to meteorologically dependent data, more years should be simulated.

5. Conclusions

Despite the relatively high potential for offshore wind generation in Japan, this resource is less developed than other RES-E, in part because turbines that are currently on the market do not generate efficiently or at all during typhoon events. In this study, the authors expanded the EnSym model to simulate offshore wind electricity generation and integration potential for the estimated wind resource of Japan (91 GW) as part of the energy mix by 2030. In doing so, the authors made three observations:

- While the target capacity for offshore wind in 2030 according to the 6th SEP is 10 GW, the resource could be effectively integrated into the energy system even at 91 GW capacity without reinforcement of the existing onshore transmission grid. This suggests that an even higher capacity development target could safely be set for 2030.
- The introduction of T-class turbines to Japan could significantly increase the wind generation share in the energy mix.
- A focus on developing offshore wind off the coast of high-demand and well-connected regions could improve opportunities for the integration of this resource into the energy mix compared to the current policy strategy, which seems to focus more on development in regions with high resource potential. However, for uses that do not depend on transmission grid integration, such as electrolysis directly on-site, Hokkaido and Kyushu may be highly efficient regions to develop offshore wind capacity.

Acknowledgements

A part the present work was performed as a part of activities of Research Institute of Sustainable Future Society, Waseda Research Institute for Science and Engineering, Waseda University. This research was supported by Japan Science and technology Agency (JST) as part of the Belmont Forum Grant Number JPMJBF18T2.

Conflict of interest

The authors declare no conflicts of interest.

References

1. United Nations Framework Convention on Climate Change (UNFCCC) (2016) Paris Agreement. Available from: https://unfccc.int/sites/default/files/english_paris_agreement.pdf.
2. Intergovernmental Panel on Climate Change (IPCC) (2015) Climate change 2014 mitigation of climate change: Summary for policymakers and technical summary. Available from: https://www.ipcc.ch/site/assets/uploads/2018/03/WGIIIAR5_SPM_TS_Volume-3.pdf.
3. Kawakami A (2020) Suga's 2050 zero-carbon goal thrusts Japan into green tech race. *NIKKEI Asia*. Available from: <https://asia.nikkei.com/Spotlight/Environment/Suga-s-2050-zero-carbon-goal-thrusts-Japan-into-green-tech-race>.
4. Ministry of Economy, Trade and Industry (METI) (2021) Outline of 6th Strategic Energy Plan. Available from: https://www.enecho.meti.go.jp/en/category/others/basic_plan/pdf/6th_outline.pdf.
5. Agency for Natural Resources and Energy (ANRE) (2018) Japan's strategic energy plan. Available from: <https://www.numo.or.jp/topics/1-1Nakanishi.pdf>.
6. Ministry of Economy, Trade and Industry (METI) (2021) Japan's energy 2020—10 questions for understanding the current energy situation. Available from: https://www.enecho.meti.go.jp/en/category/brochures/pdf/japan_energy_2020.pdf.
7. Kato J (2020) Initiatives to make offshore wind power the primary power source. *JWPA*. Available from: <https://reglobal.co/wp-content/uploads/2021/01/Offshore-Wind-in-Japan.pdf>.
8. Ministry of Economy, Trade and Industry (METI)(2020) Methods of the METI for the realization of a hydrogen society. Available from: https://www.env.go.jp/seisaku/list/ondanka_saisei/lowcarbon-h2-sc/events/PDF/shiryoku06.pdf.
9. Hokkaido Government (2020) Hokkaido hydrogen society realization strategy vision. Available from: https://www.pref.hokkaido.lg.jp/fs/5/6/0/1/2/5/1/_/suisovisionkaiteiban_soan.pdf.
10. METI Kyushu (2022) Kyushu hydrogen guidebook. Available from: https://www.kyushu.meti.go.jp/seisaku/kankyojirei/2022_hydrogen/pdf/1_all.pdf.
11. Kimura K (2018) Analysis of wind power costs in Japan. *Renewable Energy Institute (Renewable EI)*. Available from: https://www.renewable-ei.org/en/activities/reports/img/pdf/20180125/JapanWindPowerCostReport_EN_20180124.pdf.
12. Ishihara T, Yamaguchi A, Takahara K, et al. (2005) An analysis of damaged wind turbines by typhoon Maemi in 2003. *The Sixth Asia-Pacific Conference on Wind Engineering*. Available from: <file:///C:/Users/User/Downloads/Turbine-Damage-Maemi-Typhoon-Analysis.pdf>.
13. Chen X, Xu JZ (2016) Structural failure analysis of wind turbines impacted by super typhoon Usagi. *Engineering Failure Analysis*. 60: 391–404. <https://doi.org/10.1016/j.engfailanal.2015.11.028>
14. Siemens Gamesa offshore. Available from: <https://www.siemensgamesa.com/products-and-services/offshore>.
15. Vestas V174-9.5 MW turbine. Available from: <https://www.vestas.com/en/products/offshore/v174-9-5-mw->
16. Vestas V236-15 MW turbine. Available from: <https://www.vestas.com/en/products/offshore/V236-15MW>.
17. Durakovic A (2021) MingYang launches 16 MW offshore wind turbine. Available from: <https://www.offshorewind.biz/2021/08/20/mingyang-launches-16-mw-offshore-wind-turbine/>.

18. IECRE-Renewable Energy (2022) Type Certificate RNA—Rotor Nacelle Assembly. Adapted to offshore wind conditions, issued to General Electric Renovables España. Available from: <https://certificates.iecre.org/#/deliverables/CERT/1587187/view>.
19. Energy Northern Perspective (2021) Siemens Gamesa to install first of its SG 11.0-200 DD machines at Ørsted's Gode Wind 3. Available from: <https://energynorthern.com/2021/12/20/siemens-gamesa-to-install-first-of-its-sg-11-0-200-dd-machines-at-orsted-s-gode-wind-3/>.
20. Lague P (2020) MHI Vestas installs flagship V174-9.5 MW prototype. *Power Eng Int*. Available from: <https://www.powerengineeringint.com/renewables/mhi-vestas-installs-flagship-v174-9-5-mw-prototype/>.
21. Durakovic A (2021) SG 11.0-200 DD turbine model secures full type certificate early. *offshoreWIND.biz*. Available from: <https://www.offshorewind.biz/2021/05/31/sg-11-0-200-dd-turbine-model-secures-full-type-certificate-early/>.
22. Durakovic A (2021) Vestas 15 MW prototype offshore wind turbine to spin in Denmark. *offshoreWIND.biz*. Available from: <https://www.offshorewind.biz/2021/10/15/vestas-15-mw-prototype-offshore-wind-turbine-to-spin-in-denmark/>.
23. Nehls G (2021) MingYang Smart Energy launches MySE 16.0-242 offshore hybrid drive wind turbine. *CompositesWorld*. Available from: <https://www.compositesworld.com/news/mingyang-smart-energy-launches-myse-160-242-offshore-hybrid-drive-wind-turbine>.
24. Energy Rich Japan Report (2003) Available from: www.energyrichjapan.info.
25. Esteban M, Zhang Q, Utama A, et al. (2010) Methodology to estimate the output of a dual solar-wind renewable energy system in Japan. *Energy Policy* 38: 7793–7802. <https://doi.org/10.1016/j.enpol.2010.08.039>
26. Esteban M, Zhang Q, Utama A (2012) Estimation of the energy storage requirement of a future 100% renewable energy system in Japan. *Energy Policy* 47: 22–31. <https://doi.org/10.1016/j.enpol.2012.03.078>
27. Esteban M, Portugal Pereira J (2014) Post-disaster resilience of a 100% renewable energy system in Japan. *Energy* 68: 756–764. <https://doi.org/10.1016/j.energy.2014.02.045>
28. Esteban M, Portugal Pereira J, Mclellan BC, et al. (2018) 100% renewable energy system in Japan: Smoothing and ancillary services. *Appl Energy* 224: 698–707. <https://doi.org/10.1016/j.apenergy.2018.04.067>
29. Wakiyama T, Kuriyama A (2018) Assessment of renewable energy expansion potential and its implications on reforming Japan's electricity system. *Energy Policy* 115: 302–316. <https://doi.org/10.1016/j.enpol.2018.01.024>.
30. Yoshihara K, Ohashi H (2017) Assessing the impact of renewable energy sources: Simulation analysis of the Japanese electricity market. *Research Institute of Economy, Trade and Industry*. Discussion Paper Series 17-E-063. Available from: <https://www.rieti.go.jp/en/publications/summary/17040014.html>.
31. Knüpfer K, Rogalski N, Knüpfer A, et al. (2022) A reliable energy system for Japan with merit order dispatch, high variable renewable share and no nuclear power. *Appl Energy* 328. <https://doi.org/10.1016/j.apenergy.2022.119840>
32. Tsuchiya H (2012) Electricity supply largely from solar and wind resources in Japan. *Renewable Energy* 48: 318–325. <https://doi.org/10.1016/j.renene.2012.05.011>

33. Heard BP, Brook BW, Wigley TML, et al. (2017) Burden of proof: A comprehensive review of feasibility of 100% renewable-electricity systems. *Renewable Sustainable Energy Rev* 76: 1122–1133. <https://doi.org/10.1016/j.rser.2017.03.114>
34. Ministry of Economy, Trade and Industry (METI) (2021) About renewable energy in 2030. Available from: https://www.meti.go.jp/shingikai/enecho/denryoku_gas/saisei_kano/pdf/031_02_00.pdf.
35. Organization for Cross-regional Coordination of Transmission Operators (OCCTO) (2019) Aggregation of electricity supply plans, Fiscal Year 2019, Figure 3–4: Composition of installed power generation capacity for each regional service area. Available from: http://www.occto.or.jp/en/information_disclosure/supply_plan/files/supplyplan_2019.pdf.
36. Agency for Natural Resources and Energy (ANRE) (2022) Website of the introduction status of renewable energy electricity. Available from: <https://www.fit-portal.go.jp/PublicInfoSummary>.
37. Japan Atomic Industrial Forum (JAIF) (2019) Current status of nuclear power plants in Japan. Available from: https://www.jaif.or.jp/cms_admin/wp-content/uploads/2019/12/jp-npps-operation20191205_en.pdf.
38. Knüpfer K, Dumlao SMG, Esteban M, et al. (2021) Analysis of PV subsidy schemes, installed capacity and actual generation in Japan from 1994 to 2019. *Energies* 8: 2128. <https://doi.org/10.3390/en14082128>
39. Ministry of Economy, Trade and Industry (METI) (2020) Overview of the vision for offshore wind power industry. Available from: https://www.meti.go.jp/shingikai/energy_environment/yojo_furyoku/pdf/002_02_e01_01.pdf.
40. Department of Energy (DOE) (2020) Global Energy storage database. Available from: <https://sandia.gov/ess-ssl/gesdb/public/index.html>.
41. Japan Meteorological Agency (JMA) (2020) Past meteorological data download landing page. Available from: <https://www.data.jma.go.jp/gmd/risk/obsdl/index.php>.
42. Japan Meteorological Agency (JMA) (2021) List of regional meteorological measurement station. Available from: https://www.jma-net.go.jp/common/catalogue/format/ObdObs_Amedas_ObsList_format.pdf.
43. Dhar A, Naeth MA, Jennings PD, et al. (2020) Geothermal energy resources: potential environmental impact and land reclamation. *Environ Rev* 28: 415–427. <https://doi.org/10.1139/er-2019-0069>
44. USACE, USFWS (2008) Hydropower rehabilitations, dissolved oxygen and minimum flow at Wolf Creek Dam, Kentucky and Center hill and dale hollow dams, Tennessee. Draft Environmental Impact Assessment, 13. Available from: <https://books.google.co.jp/books?id=nQMzAQAAMAAJ&printsec=frontcover&hl=ja#v=onepage&q&f=false>.
45. Agency for Natural Resources and Energy (ANRE) (2020) Power survey statistics of 2020. Available from: https://www.enecho.meti.go.jp/statistics/electric_power/ep002/pdf/2020/0-2020.pdf.
46. TEPCO (2020) Hourly demand progress. Available from: <https://www.tepco.co.jp/en/forecast/html/download-e.html>.

-
47. Kainou K (2016) Development of policy impact assessment model for the regulatory reform policy of Japanese electricity market. *Research Institute of Economy, Trade and Industry*. Discussion Paper Series 16-J-012. Available from: <https://www.rieti.go.jp/jp/publications/dp/16j012.pdf>.
 48. Japan Atomic Industrial Forum (JAIF) (2022) Current status of nuclear power plants in Japan. Available from: https://www.jaif.or.jp/cms_admin/wp-content/uploads/2022/04/2022-02.pdf.
 49. JPOWER (2022) Geothermal Power Generation Business. Available from: https://www.jpowers.co.jp/bs/renewable_energy/geothermal/.
 50. Japan Organization for Metals and Energy Security (JOGMEC) (2019) Geothermal in Japan. Available from: https://geothermal.jogmec.go.jp/information/plant_japan/.

Appendix

Nuclear power target capacity adjustment from 38 GW to 33.2 GW.

Based on the list of current status of nuclear plants provided by the Japan Atomic Industrial Forum [48], Table A1 lists the power plants which currently under operation and expect to be working in 2030 (some of which may eventually have their working life extended over 60 years).

Table A1. Installed nuclear capacity (MW) assumed to be available in 2030 by region (Source: JAIF [48]).

Plant name	Owner	Location	Capacity
TOKAI-2	JAPC	Kanto	1100
TSURUGA-2	JAPC	Hokuriku	1160
TOMARI-1	Hokkaido EPC	Hokkaido	579
TOMARI-2	Hokkaido EPC	Hokkaido	579
TOMARI-3	Hokkaido EPC	Hokkaido	912
ONAGAWA-2	Tohoku EPC	Tohoku	825
ONAGAWA-3	Tohoku EPC	Tohoku	825
HIGASHIDORI-1	Tohoku EPC	Tohoku	1100
KASHIWAZAKI KARIWA-1	TEPCO	Hokuriku	1100
KASHIWAZAKI KARIWA-2	TEPCO	Hokuriku	1100
KASHIWAZAKI KARIWA-3	TEPCO	Hokuriku	1100
KASHIWAZAKI KARIWA-4	TEPCO	Hokuriku	1100
KASHIWAZAKI KARIWA-5	TEPCO	Hokuriku	1100
KASHIWAZAKI KARIWA-6	TEPCO	Hokuriku	1356
KASHIWAZAKI KARIWA-7	TEPCO	Hokuriku	1356
HAMAOKA-3	Chubu EPC	Chubu	1100
HAMAOKA-4	Chubu EPC	Chubu	1137
HAMAOKA-5	Chubu EPC	Chubu	1380
SHIKA-1	Hokuriku EPC	Hokuriku	540
SHIKA-2	Hokuriku EPC	Hokuriku	1358
MIHAMA-3	Kansai EPC	Hokuriku	826
TAKAHAMA-1	Kansai EPC	Hokuriku	826
TAKAHAMA-2	Kansai EPC	Hokuriku	826
TAKAHAMA-3	Kansai EPC	Hokuriku	870
TAKAHAMA-4	Kansai EPC	Hokuriku	870
OHI-3	Kansai EPC	Hokuriku	1180
OHI-4	Kansai EPC	Hokuriku	1180
SHIMANE-2	Chugoku EPC	Chugoku	820
IKATA-3	Shikoku EPC	Shikoku	890
GENKAI-3	Kyushu EPC	Kyushu	1180
GENKAI-4	Kyushu EPC	Kyushu	1180
SENDAI-1	Kyushu EPC	Kyushu	890
SENDAI-2	Kyushu EPC	Kyushu	890
Total operable capacity:			33,235

Planned geothermal regional capacity development projects to 2030

There are five geothermal plants, totaling 66.1 MW, that are scheduled to connect to the energy system by 2030, as shown in Table A2. Based on this information, additional capacity was added to Hokkaido and Tohoku individually, while the remaining was distributed proportionally amongst regions.

Table A2. Geothermal power plants planned to operate before 2030 (JPOWER [49]; JOGMEC [50]; METI [34]).

Project name	Region	Planned capacity (MW)	Planned start date	Developer
Minamikayabe	Hokkaido	6.5	2022	FIT
Onikoube	Tohoku	14.9	2023	JPOWER
Appi	Tohoku	14.9	2024	JPOWER
Oyasu	Tohoku	14.9	2026	FIT
Kijiyama	Tohoku	14.9	2029	FIT

Solar and wind data measurement stations

Table A3 lists the locations and station IDs used to measure solar and wind potential generation [41,42].

Table A3. List of JMA station IDs by prefecture and resource (Source: JMA [41,42]).

Prefecture	Onshore wind	Offshore wind	Solar
Hokkaido	s47420	24101	a0047
Aomori	a1122		s47581
Akita	a0186	32616	a0183
Iwate	a0211		a0236
Yamagata	a1465		s47520
Miyagi	a1626		s47590
Fukushima	s47570		a1034
Tochigi	s47615		a0335
Ibaraki	s47629		s47629
Saitama	s47626		s47626
Gunma	s47624		a1021
Chiba	s47648		a0376
Tokyo	a0371	44226	a0370
Kanagawa	a0392		a1443
Yamanashi	s47638		a1023
Shizuoka	s47655	50506	a0451
Niigata	a1469	54166	s47604
Nagano	a0399		a0399
Toyama	a1533		s47606
Fukui	a1071		s47616
Ishikawa	s47600		s47605
Gifu	a0493		s47632
Mie	a1230		a0509
Aichi	a0470		a0984
Shiga	a0586		a0963
Nara	a0635		s47780
Wakayama	a1485	65036	s47778
Osaka	a1471		s47772
Kyoto	s47750		s47750
Hyogo	s47776		s47770
Kagawa	s47891		s47891
Tokushima	s47895		a1242
Kochi	s47898	74271	a1249
Ehime	a1456		a0739
Tottori	a1519		a1231
Shimane	s47755		a0704
Okayama	s47768		a0668
Hiroshima	a0686	67511	a0686

Continued on next page

Prefecture	Onshore wind	Offshore wind	Solar
Yamaguchi	a0779		a0775
Fukuoka	a0943		a0943
Saga	a1610		a0829
Kumamoto	a1240		a0834
Nagasaki	s47805	84072	a0922
Oita	s47814		a1237
Miyazaki	s47822	87492	s47822
Kagoshima	a0895		s47827

T-class turbine

The Vestas model V236-15MWTM was chosen as it is classified as an S and T-class turbine, which can stand severe weather conditions such as typhoons. Further, among turbines at this capacity, it had the most publicly available information, such as cut-in and cut-out speed and rotor diameter. The authors estimated a power curve for the model through approximation from the Vestas V100/1.8 turbine, which was chosen due to the public availability of its power curve and due to it being produced by the same manufacturer.

As the cut-in speed of the two turbines is different, the power of the V236-15MW at its cut-in speed (3 m/s) was calculated by extrapolation:

Hourly wind generation [E_{wind} (Wh)] is given by:

$$E_{wind} = \frac{1}{2} \rho A_w V^3 C_p \quad (1)$$

where ρ is air density which assumed as $1.225 \frac{kg}{m^3}$, A_w is the wind-swept area [m^2], V is the wind velocity [$(\frac{m}{s})^3$] and C_p is the power coefficient.

By substituting this information into the generation equation, a C_p value at 3.5 and 4 m/s can be obtained:

$$E_{wind}[Wh] = \frac{1}{2} \rho A_w V^3 C_p \quad (2)$$

$$413[kWh] \times 1000 = \frac{1}{2} \times 1.225 \times 43742 \times 3.5^3 \times C_{p_{3.5}} \quad (3)$$

$$C_{p_{3.5}} = 0.571 \quad (4)$$

$$876[kWh] \times 1000 = \frac{1}{2} \times 1.225 \times 43742 \times 4^3 \times C_{p_{4.0}} \quad (5)$$

$$C_{p_{4.0}} = 0.763 \quad (6)$$

Next, the C_p value at 3 m/s is estimated by extrapolating:

$$C_{p_{3.0}} = \frac{0.5C_{p_{4.0}} - C_{p_{3.5}}}{-0.5} = \frac{0.5 \times 0.763 - 0.571}{-0.5} = 0.38 \quad (7)$$

After obtaining the C_p value at 3 m/s, the potential generation at 3 m/s can be estimated:

$$E_{wind} = \frac{1}{2} \times 1.225 \times 43742 \times 3^3 \times 0.38 = 274800[Wh] = 274.8[kWh] \quad (8)$$

Based on the potential generation estimated for 3 m/s, the potential generation for the wind speed from 3.5 to 20 m/s is obtained proportionately to the V100/1.8 turbine. Wind speeds between 20 m/s and 30 m/s can generate full power on the V236-15MW turbine. The advantage of a such a turbine is not only that it can withstand typhoons, but that it can also produce power at high cut-out speeds at a high nominal rating. This power curve is summarized in Table A4.

Table A4. Power curve data of Vestas turbines.

Turbine	Vestas 1.8	Vestas 15.0
Capacity [kW]	1815	15000
Wind speed [m/s]	Power [kWh]	
0.00	0	0
1.50	0	0
2.00	0	0
2.50	0	0
3.00	0	275
3.50	50	413
4.00	106	876
4.50	173	1,430
5.00	248	2,050
5.50	338	2,793
6.00	443	3,661
6.50	556	4,595
7.00	705	5,826
7.50	873	7,215
8.00	1,063	8,785
8.50	1,269	10,488
9.00	1,474	12,182
9.50	1,641	13,562
10.00	1,744	14,413
10.50	1,792	14,810
11.00	1,808	14,942
11.50	1,814	14,992
12.00	1,815	15,000
12.50	1,815	15,000
13.00	1,815	15,000
13.50	1,815	15,000
14.00	1,815	15,000
14.50	1,815	15,000
15.00	1,815	15,000
15.50	1,815	15,000
16.00	1,815	15,000
16.50	1,815	15,000
17.00	1,815	15,000
17.50	1,815	15,000
18.00	1,815	15,000
18.50	1,815	15,000
19.00	1,815	15,000
19.50	1,815	15,000
20.00	1,815	15,000
20.50	0	15,000
21.00	0	15,000
21.50	0	15,000

Continued on next page

Turbine	Vestas 1.8	Vestas 15.0
Capacity [kW]	1815	15000
Wind speed [m/s]	Power [kWh]	
22.00	0	15,000
22.50	0	15,000
23.00	0	15,000
23.50	0	15,000
24.00	0	15,000
24.50	0	15,000
25.00	0	15,000
25.50	0	15,000
26.00	0	15,000
26.50	0	15,000
27.00	0	15,000
27.50	0	15,000
28.00	0	15,000
28.50	0	15,000
29.00	0	15,000
29.50	0	15,000
30.00	0	15,000

Based on these values, the power curve for the V236-15MWTM is shown in Figure A1, as compared with the power curve of the V100/1.8 turbine.

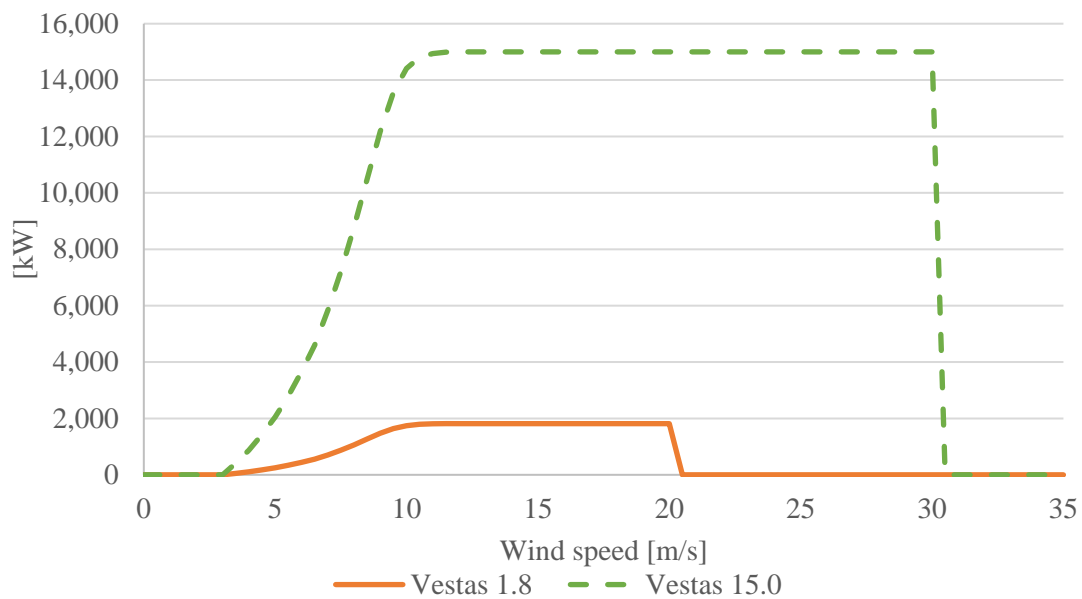


Figure A1. Power curve of Vestas turbine models.

Submarine cable parameter

Table A5. Information of submarine cable.

Parameter	Material/ Value
Cable type	XLPE (cross linked polyethylene)
Core number	3
Voltage [kV]	220
Cross-section area [mm ²]	800



AIMS Press

© 2023 the Author(s), licensee AIMS Press. This is an open access article distributed under the terms of the Creative Commons Attribution License (<http://creativecommons.org/licenses/by/4.0>)